Addendum to the MiniBooNE Run Plan: Continued AntiNeutrino Running in 2007

September 25, 2006

A. A. Aguilar-Arevalo[5], S. J. Brice[7], B. C. Brown[7], L. Bugel[5], J. M. Conrad[5], D. Cox[8], A. Curioni[16], Z. Djurcic[5], D. A. Finley[7], B. T. Fleming[16], R. Ford[7], F. G. Garcia[7], G. T. Garvey[9], A. Green[8], C. Green[9], E. Hawker[15], R. Imlay[10], R. A. Johnson[3], P. Kasper[7], T. Katori[8], T. Kobilarcik[7], I. Kourbanis[7], S. Koutsoliotas[2], J. M. Link[14], Y. Liu[1], W. C. Louis[9], K. Mahn[5], W. Marsh[7], G. McGregor[9], S. McKenney[9], W. Metcalf[10], H. O. Meyer[8], P. D. Meyers[12], G. B. Mills[9], J. Monroe[5], C. Moore[7], R. H. Nelson[4], P. Nienaber[13], S. A. Ouedraogo[10], R. B. Patterson[12], C.C. Polly[8], E. Prebys[7], J. L. Raaf[3], H. Ray[9], B. P. Roe[11], A. D. Russell[7], R. Schirato[9], D. Schmitz[5], M. H. Shaevitz[5], F. C. Shoemaker[12], D. Smith[6], M. Sorel[5], P. Spentzouris[7], I. Stancu[1], R. Stefanski[7], H. A. Tanaka[12], R. Tayloe[8], M. Tzanov[4], R. Van de Water[9], M. O. Wascko[10*], D. H. White[9], M. Wilking[4], H. J. Yang[11], G. P. Zeller[5], E. D. Zimmerman[4]

[1] *University of Alabama*
[2] *Bucknell University*
[3] *University of Cincinnati*
[4] *University of Colorado*
[5] *Columbia University*
[6] *Embry Riddle Aeronautical University*
[7] *Fermi National Accelerator Laboratory*
[8] *Indiana University*
[9] *Los Alamos National Laboratory*
[10] *Louisiana State University*
[11] *University of Michigan*
[12] *Princeton University*
[13] *St. Mary's University of Minnesota*
[14] *Virginia Polytechnic Institute and State University, Blacksburg*
[15] *Western Illinois University*
[16] *Yale University*
[*] *Now at Imperial College, London*

Contents

Chapter 1

Executive Summary

The primary physics goal of MiniBooNE is to confirm or rule out the LSND $\bar{\nu}_\mu \to \bar{\nu}_e$ oscillation observation with high significance. In the 2003 Run Plan document [1] presented to the PAC we outlined the need for 1×10^{21} protons on target (POT) to achieve this goal. In fall 2004 we expanded this run plan to add antineutrino running, requesting further running with reverse horn polarity [2]. In this document, which is largely an update of the fall 2004 plan, we express the importance of completing the antineutrino running that began in early 2006, taking us into FY2007.

In January of 2006, based on our run plan, we switched horn polarity to begin running in antineutrino mode. We currently have collected 1.0×10^{20} POT. Based on the labs projections of delivering $1 - 2 \times 10^{20}$ POT in FY2006, our fall 2004 request was based on the physics possible with 2×10^{20} POT. Our current plan is to finish this run by collecting a further 1×10^{20} POT, to give a total of 2×10^{20} POT in antineutrino mode. This doubling in statistics will ensure our ability to carry out the physics goals we envision.

The $\nu_\mu \to \nu_e$ appearance analysis is currently in progress, and we anticipate having a result soon. The outcome of this result could change how we want to define further running, e.g. neutrino mode, 25m absorber, etc. However, the current request is that we complete the present run program before considering new run modes. Assuming NuMI running we can collect about $\sim 1 \times 10^{19}$ POT per month. Thus, by the next shutdown (June 2007) we can collect a further $\sim 1 \times 10^{20}$ POT, which brings us to our goal of 2×10^{20} POT total.

As this document will show, MiniBooNE antineutrino running will produce significant new physics results, including a $\bar{\nu}_\mu$ disappearance oscillation search and the world's only $\bar{\nu}_\mu$ cross section measurements in this energy region. The sensitivity of the $\bar{\nu}_\mu$ disappearance oscillation analysis extends an order of magnitude lower than the current bound of $\Delta m^2 \sim 10\,\mathrm{eV}^2$. Cross section measurements of $\bar{\nu}_\mu$ charged current quasi-elastic scattering and single pion production, where current uncertainties are greater than 30%, can be made with better than 10% statistical precision. Of crucial importance is the NC π^0 mode, improved production rate measurement as a function of energy will allow a better determination of the electron misidentification background rates, which is of keen interest to future long baseline experiments such as T2K and NOνA.

This continuation of antineutrino running may also serve as the first installment

of a longer run that would complete the process of checking the LSND result, which was seen in antineutrino interactions. These physics goals were identified as strong priorities by the recent APS Interdivisional Neutrino Study [3], reflecting the broad interest of the neutrino community.

On the basis of the compelling physics case presented in this document, we ask the PAC to endorse that:

- A further 1×10^{20} POT in anti-neutrino mode be delivered to MiniBooNE, which would extend current running into FY2007.
- Higher proton intensity continue to be vigorously pursued.

We also would like the opportunity to present a new run plan at the spring 2007 PAC review based on the outcome of the on going neutrino appearance analysis.

Chapter 2

Current Antineutrino Running

2.1 Run Performance

Starting in early January 2006, a two week shutdown of MiniBooNE operations occurred to swap out the positive charging supplies and replace them with negative supplies. Work also was done to the power bus to make future change outs easier and quicker, reducing a two week job to less than one week. The power supply change out was successful and on January 18, 2006 we began operations with a reversed horn current of -175kA, focusing negative charged particles, which preferentially produce antinuetrinos and a roughly 30% admixture of neutrinos.

Figure 2.1 shows the weekly performance since the start of running in 2002. The antineutrino running is shown after the dotted line; the large gap is the 2006 March shutdown which lasted three months. The performance of the Booster after the shutdown took some time to ramp up, but during August we reached the Champagne goal of 9×10^{16} protons/hr for one hour, and the 1.08×10^{19} protons delivered in the week broke the weekly-integrated proton record.

These milestones were due to the outstanding work of the Accelerator Division pushing the Booster to peak performance. This has resulted in an impressive total of 1.0×10^{20} POT delivered to MiniBooNE in the five months since the start of antineutino running in January 2006. The overall performance is demonstrated in Figure 2.2 which shows the integrated protons on target delivered to the MiniBooNE beamline from Jan 18, 2006 to Sept 11, 2006.

Over half the integrated data was collected while NuMI was down, which increases our instaneous rates by about a factor of four. This can be seen in Figure 2.1 as two high intensity bumps in the POT plot. During normal running, i.e. NuMI is on, we expect a weekly average of about 0.3×10^{19} POT. This translates into $\sim 0.1 \times 10^{20}$ integrated POT per month, which implies ten months of running is needed to collect an extra 1×10^{20} POT. This would take us to June 2007, which is the planned start of the accelerator complex shutdown.

The bottom plot in Figure 2.1 demonstrates that the neutrinos collected per week are reduced by a factor of four relative to that of neutrino mode. This reduction is expected and further discussed in later sections.

An important aspect to continued running of MiniBooNE is the reliability of the

beamline, horn, and detector systems. During the antineutrino run period our uptime has been over 95%. The most crucial element, the horn, has collected over 100 million pulses, surpassing the first horn, which failed two years ago with 94 million pulses (both these horns have reached world records for most pulses). This second horn continues to run flawlessly with no signs of problems. In the unfortuante event of failure, we have ready a spare third horn and target. This would require three weeks to swap in, which would only be a small loss in total data.

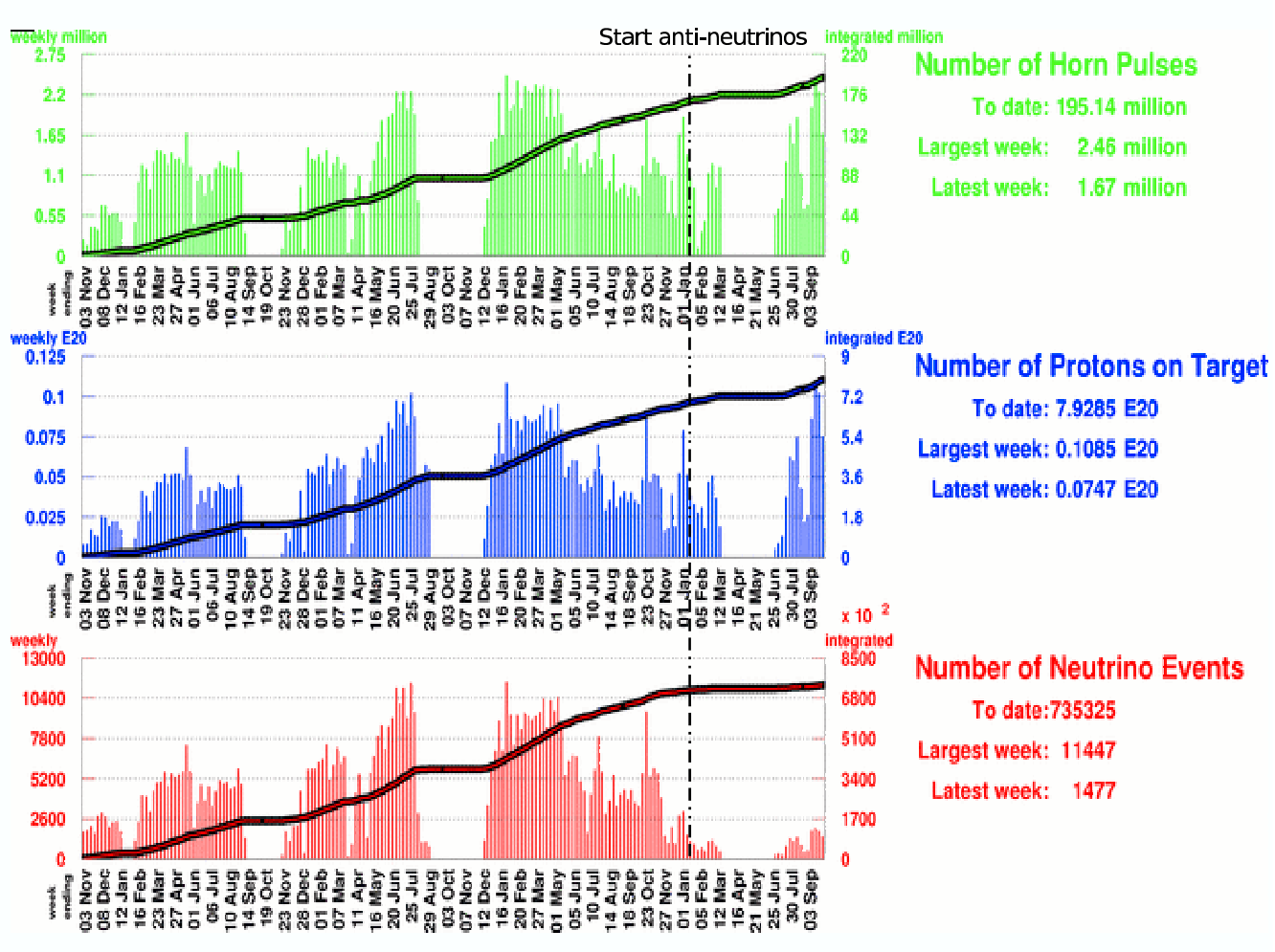

Figure 2.1: *MiniBooNE weekly run summaries from October 2002 to September 11, 2006. Top plot is number of horn pulses, the middle is protons on target, and the bottom is number of neutrino events based on simple cuts. The dashed line is the start of antineutrino running.*

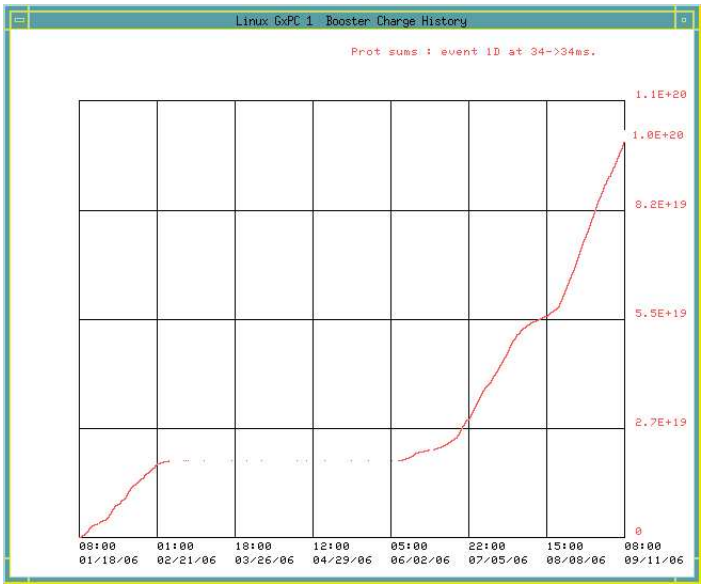

Figure 2.2: *The integrated protons on target delivered to MiniBooNE from the start of antineutrino running. The total deliverd from Jan 18, 2006 to Sept 11, 2006, is* 1×10^{20} *POT. The steep slopes are times when NuMI was off allowing us to collect three to four times the normal rate.*

2.2 Data Checks

In this section we demonstrate that the antineutrino data being collected is of good quality. Figure 2.3 shows the time window of beam triggers without any cuts, and with simple cuts to isolate neutrino candidates. The $TankHits > 200$ cut removes Michel electrons and low energy neutral current events. The $VetoHits < 6$ cut removes most incoming cosmic ray muons. What we are left with is a clean sample of antineutrino candidates, with most events falling within the 1.6 μs beam window.

Figure 2.4 shows the Charged Current Quasi Elastic (CCQE) energy with Monte Carlo overlay for a fraction of the antineutrino data set. The good agreement demonstrates that the data being taken is good, and that the underlying physics assumptions about antineutrinos are correct to first order. Also shown in Figures 2.5 and 2.6 are the reconstructed radius and UZ-cosine direction, which also have good agreement between data and Monte Carlo.

2.3 Measured AntiNeutrino Rates

To determine if the expected antineutrino rates are in agreement with what is observed, a scale factor is computed that is the ratio of data rates to our current Monte Carlo simulation. The measured antineutrino scale factor is 0.90 ± 0.01 (statistical error only) for most of the antineutrino data set collected so far. Current estimates of systematic flux errors from the neutrino analysis would cover the difference from unity. Figure 2.7 shows a plot of tank charge, which has a strong correspondence with energy, for both data and Monte Carlo absolutely normalized. The good agree-

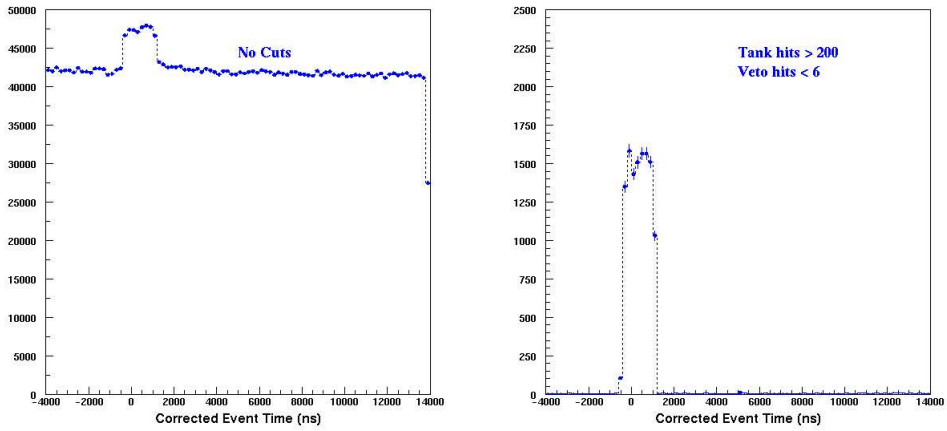

Figure 2.3: *The left plot shows the time distribution of all beam events collected within the 20 μs time window. The right plot shows the time distribution after simple antineutrino cuts, i.e. $TankHits > 200$ and $VetoHits < 6$. What remains is a strong antineutrino signal within the 1.6 μs beam spill. The data corresponds to 0.7×10^{20} POT.*

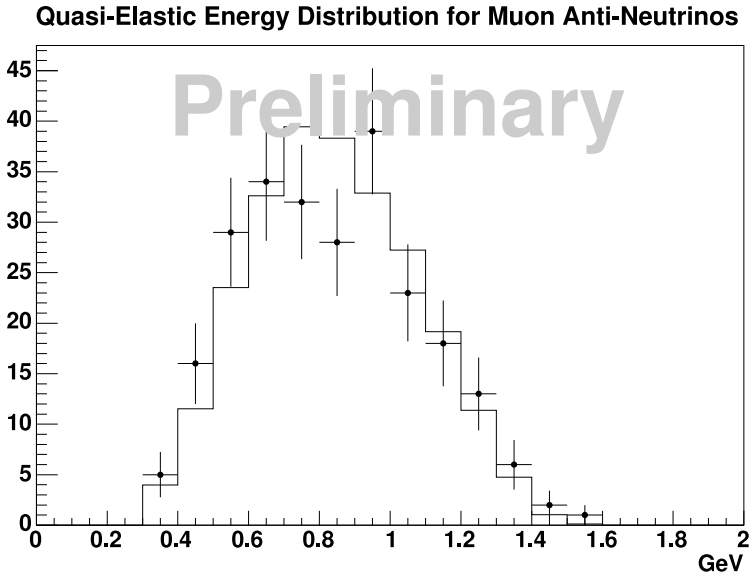

Figure 2.4: *Plot of reconstructed quasi-elastic energy for data (error bars) and Monte Carlo (solid histogram) events in $\bar{\nu}$ mode, relatively normalized. The data is from 0.5×10^{19} POT.*

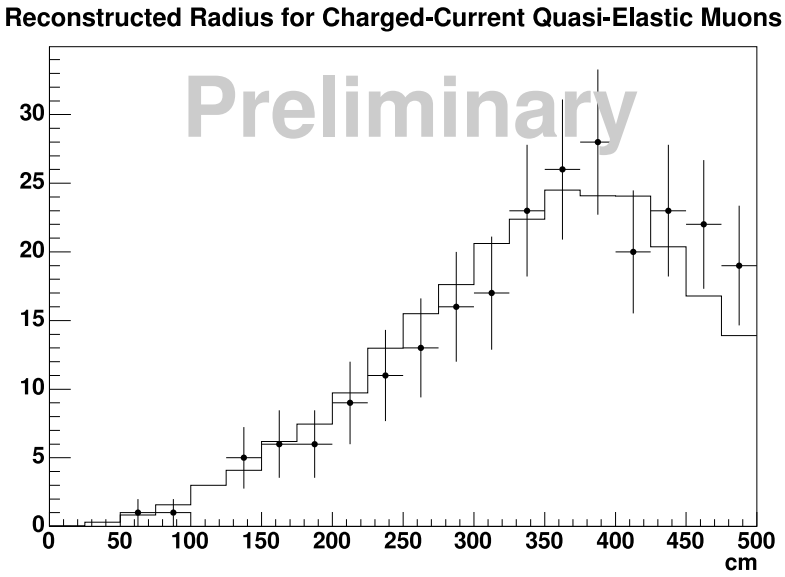

Figure 2.5: *Plot of reconstructed radius for data (error bars) and Monte Carlo (solid histogram) events in $\bar{\nu}$ mode, relatively normalized. The data corresponds to* 0.5×10^{19} *POT.*

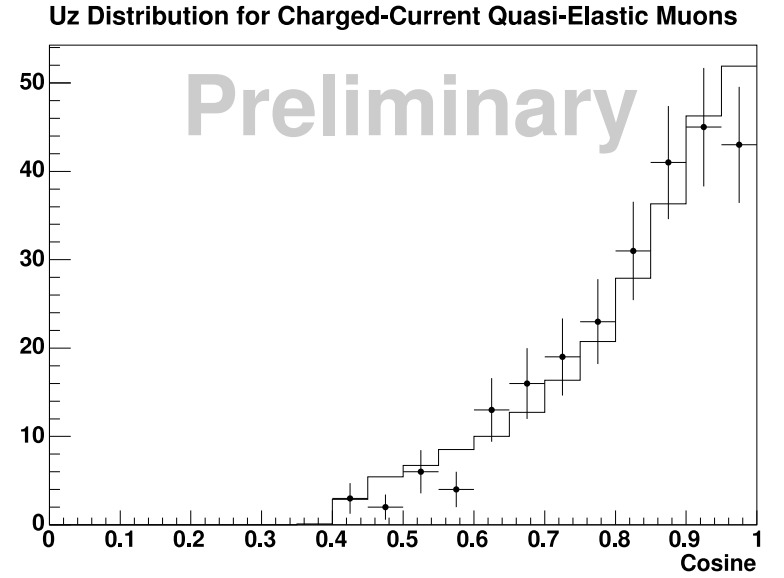

Figure 2.6: *Plot of reconstructed UZ direction for data (error bars) and Monte Carlo (solid histogram) events in $\bar{\nu}$ mode, relatively normalized. The data is from* 0.5×10^{19} *POT. The Z direction is along the beam axis.*

ment demonstrates that the observed antineutrino inclusive rates are consistent with expectation. Thus, the rates discussed later in this proposal justify the amount of data necessary to complete the antineutrino program.

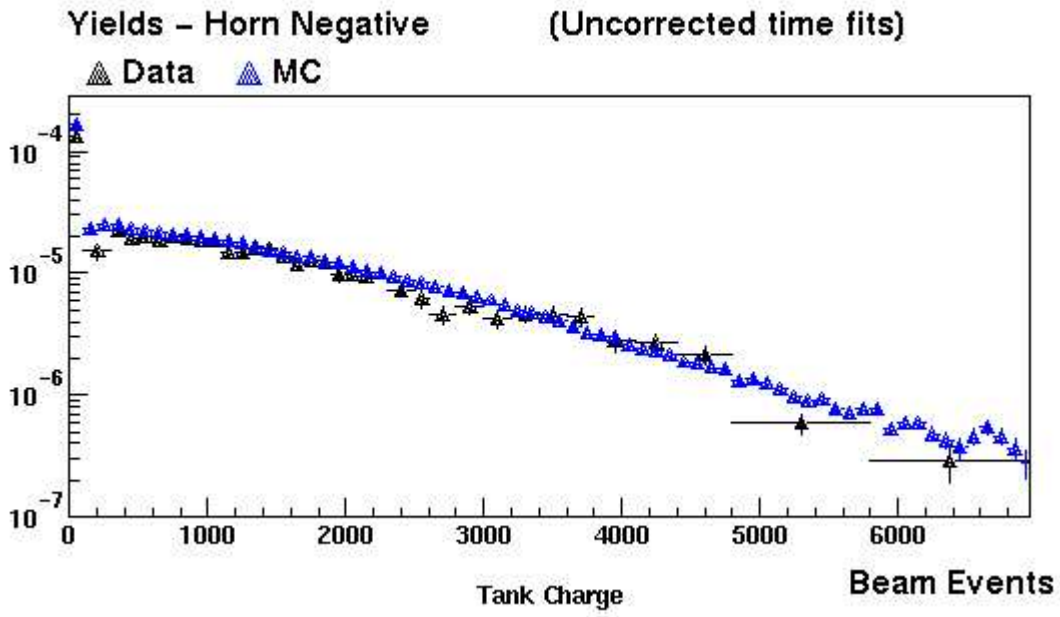

Figure 2.7: *A preliminary plot of tank charge for data events (black) and Monte Carlo events (blue), absolutely normalized. The data corresponds to* 0.7×10^{20} *POT.*

Chapter 3

Antineutrino Running in 2006

Whether MiniBooNE confirms or rules out the LSND anomaly, it is desirable for MiniBooNE to run with antineutrinos. Since the LSND result was observed with antineutrinos, it is imperative to explore the LSND signal region using antineutrinos. This would include both $\bar{\nu}_\mu$ disappearance and $\bar{\nu}_e$ appearance searches. The MiniBooNE beam line is also a unique tool for studying antineutrino cross sections at low energy, and overlaps the energy of other long baseline experiments as shown in Figure 3.1. These studies probe previously unexplored regions, thus providing key information for future programs such as T2K and NOνA. These possible cross section measurements and oscillation searches are discussed in the following two sections.

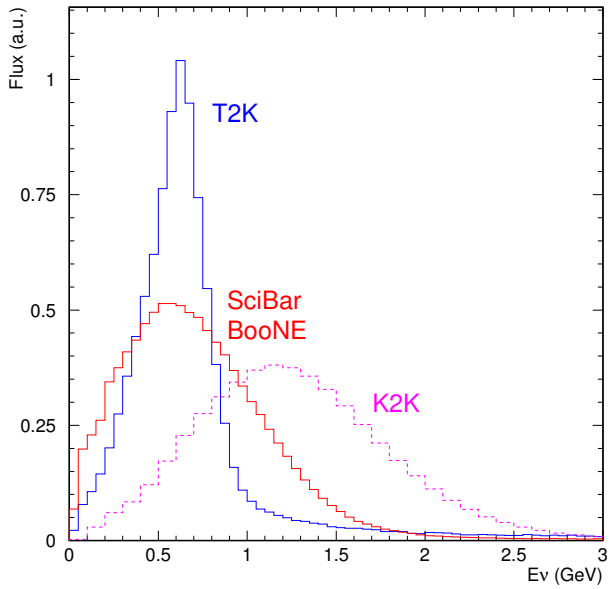

Figure 3.1: *Neutirno energy distributions for MiniBooNE/SciBooNE, compared to T2K, which shows good overlap. The expected mean energy distribution for NOνA is close to 2 GeV.*

3.1 Antineutrino Cross Section Measurements

The APS Interdivisional Neutrino Study explicitly supports the:

and recommends that the search for CP violation in neutrino oscillations be given high priority [3]. Future explorations will most likely attempt to measure CP violation by comparing oscillation probabilities for $\nu_\mu \to \nu_e$ versus $\bar{\nu}_\mu \to \bar{\nu}_e$. To accomplish this, one needs control of the ratio of $\nu/\bar{\nu}$ cross sections to a better precision than the size of the expected asymmetry. In addition, if such measurements are to be made using a nuclear target to maximize event statistics, the antineutrino cross sections cannot simply be inferred from the neutrino cross sections since the nuclear effects for neutrino and antineutrino interactions are not identical. Figure 3.2 compares the size of the expected nuclear effects for neutrino and antineutrino quasi-elastic (QE) interactions on carbon. As a result of a softer Q^2 distribution, the antineutrino cross section reduction is roughly $20-30\%$ larger than for neutrino scattering.

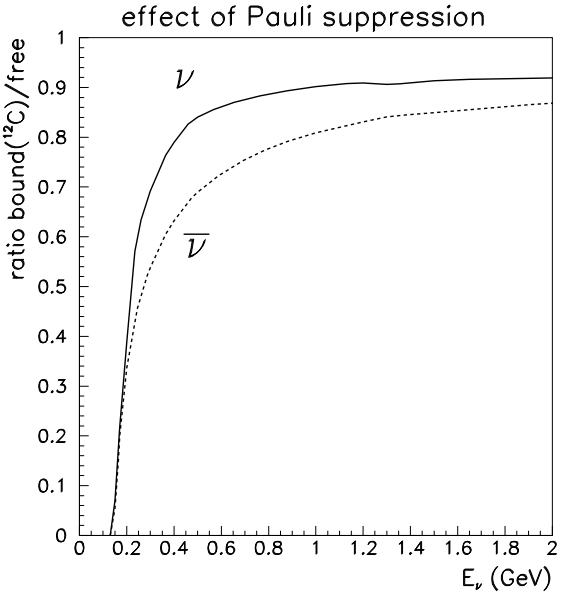

Figure 3.2: *Size of the estimated nuclear effects for ν (solid) and $\bar{\nu}$ (dashed) CC QE interactions on carbon as a function of neutrino energy. Predictions are from the NUANCE Monte Carlo generator [7].*

While published low energy neutrino cross section data are hardly copious [8], measurements of low energy antineutrino cross sections are even *more* scarce. Additional antineutrino data on nuclear targets are clearly needed so that interaction spectra and background rates for antineutrino oscillation experiments (including our own) can be estimated with confidence. Fermilab, through MiniBooNE, can be the first to provide these necessary inputs with no additional detector cost and with the anticipated Booster proton delivery through FY2007.

3.1.1 Expected $\bar{\nu}_\mu$ Event Rates at MiniBooNE

Historically, antineutrino reactions have been more challenging to measure than neutrino reactions because accelerator-based antineutrino experiments have suffered from

lower fluxes, lower cross sections, and thus lower overall event rates. Typically, the fluxes and cross sections are each halved, leading to an overall factor of four reduction in antineutrino event rates. Antineutrino beams also have larger wrong-sign contamination than neutrino beams. In the MiniBooNE beam, antineutrinos are roughly 2% of events in neutrino running, whereas neutrinos constitute $\sim$ 30% of events in antineutrino running.

Despite the reduction in rate inherent in this and any other antineutrino beam, in just one year of running MiniBooNE expects antineutrino event statistics large enough to yield interesting and useful cross section measurements. We expect to use the same techniques to obtain a precise measure of our incoming flux in this mode as described in the MiniBooNE Run Plan [1]. Table 3.1 lists the expected antineutrino event statistics for 2×10^{20} POT at MiniBooNE. As can be seen from this table, the most abundant interactions at MiniBooNE include charged current quasi-elastic (CC QE), neutral current elastic (NC EL), resonant single-pion production, and coherent pion production processes. Rates are listed for both right-sign (antineutrino) and wrong-sign (neutrino) interactions. Note that wrong-sign interactions cannot be neglected in antineutrino running, as they can in neutrino running.

Reaction	$\bar{\nu}_\mu$ (RS) events	ν_μ (WS) events	total ($\bar{\nu}_\mu$+ν_μ)
CC QE	32,476	11,234	43,709
NC elastic	13,329	4,653	17,982
CC resonant $1\pi^-$	7,413	0	7,413
CC resonant $1\pi^+$	0	6,998	6,998
CC resonant $1\pi^0$	2,329	1,380	3,709
NC resonant $1\pi^0$	3,781	1,758	5,539
NC resonant $1\pi^+$	1,414	654	2,067
NC resonant $1\pi^-$	1,012	520	1,532
NC coherent $1\pi^0$	2,718	438	3,156
CC coherent $1\pi^-$	4,487	0	4,487
CC coherent $1\pi^+$	0	748	748
other (multi-π, DIS)	2,589	2,156	4,745
total	71,547	30,539	102,086

Table 3.1: *Event rates expected in MiniBooNE $\bar{\nu}$ running with 2×10^{20} POT assuming a 550 cm fiducial volume, before cuts. Listed are the expected right-sign (RS) and wrong-sign (WS) events for each reaction channel. These event estimates do not include the effects of final state interactions in carbon which can alter the composition of the observed final state, and do not include effects fom reconstruction.*

Given these projected statistics, which has been confirmed by the measured data to MC ratio described previously, this section describes potential cross section measurements that can be performed at MiniBooNE. First, we describe an innovative approach for measuring the wrong-sign contamination in the antineutrino data, followed by measurements of antineutrino CC QE, NC π^0, and CC single-pion cross sections.

3.1.2 Wrong Sign Constraints

Antineutrino cross section measurements, using conventional beams, must always confront a non-negligible neutrino contamination and MiniBooNE is no exception. To avoid sole reliance on beam Monte Carlo predictions, such backgrounds are commonly eliminated (at least in the case of CC interactions) by identifying the charge of the outgoing muon. Without a magnetic field to provide such event-by-event identification, MiniBooNE has developed several novel techniques for measuring wrong-sign backgrounds in the antineutrino data, allowing us to make more precise antineutrino cross section measurements. The wrong-sign content is constrained by three measurements: muon angular distributions in QE events, muon lifetimes, and CC single π^+ events. The following subsections describe each of these independent approaches.

Muon Angular Distributions

The most powerful wrong-sign constraint comes from the observed direction of outgoing muons in CC QE interactions. As can be seen from Figure 3.3, neutrino and antineutrino events exhibit distinct muon angular distributions. The final state muons in antineutrino QE interactions predominantly follow the initial neutrino direction — they are more forward peaked than muons from neutrino interactions. This same phenomenon is observed in deep inelastic scattering (DIS), in which CC antineutrino-antiquark scattering is forbidden in the backwards direction. In hadronic terms, the suppression of *antineutrino* QE scattering at backward angles arises from the destructive interference between the VA and $VV + AA$ terms in the cross section. This interference is constructive in the case of *neutrino* QE scattering. The excellent angular resolution in MiniBooNE allows us to exploit this difference and fit the angular distributions to extract the wrong-sign contribution.

Using a detailed Monte Carlo study, we find that the wrong-sign component can be reliably measured to 7% of itself after including systematic uncertainties and backgrounds. Using generated distributions, we find that the uncertainty is 5%, indicating that the resolution of the event reconstruction and background uncertainties do not significantly affect the measurement. We have also studied fits to Q^2 distributions and achieved similar results.

Muon Lifetimes

A second handle results from measuring the rate at which muons decay in the MiniBooNE detector. Due to an 8% μ^- capture probability in mineral oil, positively and negatively charged muons exhibit different effective lifetimes ($\tau \sim 2.026\,\mu s$ for μ^- [9] and $\tau \sim 2.197\,\mu s$ for μ^+ [10]). Solely using this difference, we find that the wrong-sign contribution can be extracted with a 30% statistical uncertainty and negligible systematic uncertainties. While not as precise as fits to the muon angular distributions, this particular constraint is unique, as it is independent of kinematics and reconstruction.

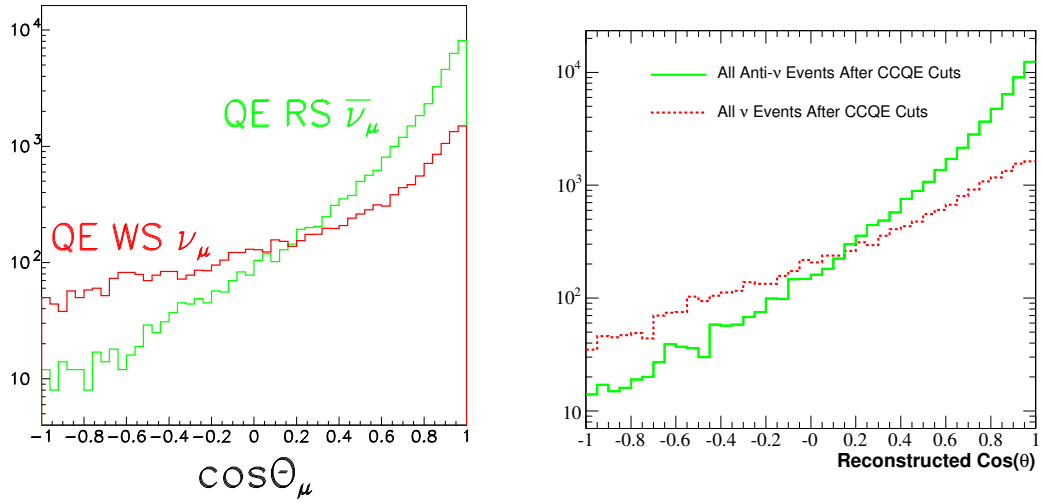

Figure 3.3: *Generated (left) and reconstructed (right) muon angular distributions for CC QE right-sign $\bar{\nu}_\mu$ and wrong-sign ν_μ interactions in antineutrino running at MiniBooNE. As in Table 3.1, neutrinos are predicted to comprise $\sim 30\%$ of the events. Unlike the lefthand plot, the righthand plot includes non-QE backgrounds. The high degree of angular separation persists even after the events have been reconstructed and have passed CC QE event selection.*

CC Single π^+ Event Sample

A third measure makes use of the fact that CC $1\pi^+$ events in antineutrino mode almost exclusively result from neutrino interactions in the detector (Table 3.1). The dominant CC single pion production channels contain a final state π^+ in the case of neutrino scattering, as opposed to a final state π^- in the case of antineutrino scattering.

MiniBooNE cleanly identifies CC $1\pi^+$ events by locating the two decay electrons that follow the primary neutrino interaction, one each from the μ^- and π^+ decay chains [11]. CC $1\pi^-$ events are largely rejected by this requirement because most of the π^-'s come to rest and are captured by carbon nuclei, resulting in no decay electrons. There is a residual background from CC $1\pi^0$ events in which the final state pion charge exchanges ($\pi^0 \rightarrow \pi^+$), but this background is estimated to be small, around 2%. The probability for double charge exchange $\pi^- \rightarrow \pi^+$ is highly suppressed, and can be completely neglected. Starting from a sample that is 70% *right-sign* antineutrino interactions, this simple two decay electron requirement yields an 85% pure sample of *wrong-sign* neutrino events (Table 3.2).

Assigning very conservative uncertainties to the antineutrino background events and the CC $1\pi^+$ cross section, which will be well-measured by the MiniBooNE neutrino data, yields a 15% uncertainty on the wrong-sign content in the beam given 2×10^{20} POT. Increased statistics yield only marginal improvement in this measurement. Gains could be made by attempting to reduce the antineutrino backgrounds in this sample; however, no such attempt to optimize the event selection was made for this initial study. This measurement is complementary to the muon angular dis-

Neutrino type	# before cuts	# after CC π^+ event selection
ν_μ (WS)	30,539	2,525
$\bar{\nu}_\mu$ (RS)	71,547	461
total	102,086	2,986

Table 3.2: *Total number of generated events compared to the number of reconstructed events passing the CC* $1\pi^+$ *selection in antineutrino running assuming* 2×10^{20} *POT.*

tribution determination because CC $1\pi^+$ events predominantly result from resonance decays, and therefore constrain the wrong-sign content at larger neutrino energies.

Summary of Wrong-Sign Measurements in the $\bar{\nu}$ Data

This set of three independent measurements (each of which have different systematics and inputs) offers a very powerful constraint on the neutrino backgrounds in antineutrino mode (Table 3.3).

Source of Measurement	WS uncertainty	resultant error on $\bar{\nu}$ cross sections
CC QE $\cos\theta_\mu$ distribution	7%	2%
CC $1\pi^+$ event sample	15%	5%
muon lifetimes	30%	9%

Table 3.3: *Wrong-sign extraction uncertainties as obtained from various independent sources in the* $\bar{\nu}$ *data. The resultant systematic uncertainty on* $\bar{\nu}$ *cross section measurements is obtained by assuming that wrong-signs comprise* 30% *of the total events.*

The resulting wrong-sign systematic on any antineutrino cross section measurement is at the 2% level, which is remarkable for a detector which does not possess event-by-event sign selection. Given this redundant approach, the wrong-sign contamination should not be considered prohibitive to producing meaningful antineutrino cross section and oscillation measurements at MiniBooNE. These techniques may also be useful for other experiments without magnetized detectors which have plans to study antineutrino interactions (*e.g.*, K2K, T2K, NOνA, Super-K).

3.1.3 CC Quasi-Elastic Scattering ($\bar{\nu}_\mu\, p \to \mu^+\, n$)

Only a handful of experimental measurements exist on antineutrino quasi-elastic scattering cross sections (Figure 3.4 and Table 3.4). All come from bubble chamber measurements that were made on a variety of target materials with limited statistics. Note, in particular, that there is a complete lack of experimental data in MiniBooNE's energy range, below 1 GeV.

To ensure the robustness of future CP violation measurements in the neutrino sector, one would prefer to avoid relying heavily on Monte Carlo predictions and extrapolations into regions where no data exist. MiniBooNE can serve an important role in this regard by making the first high statistics antineutrino QE measurement below 1 GeV. This section describes the feasibility of such a measurement.

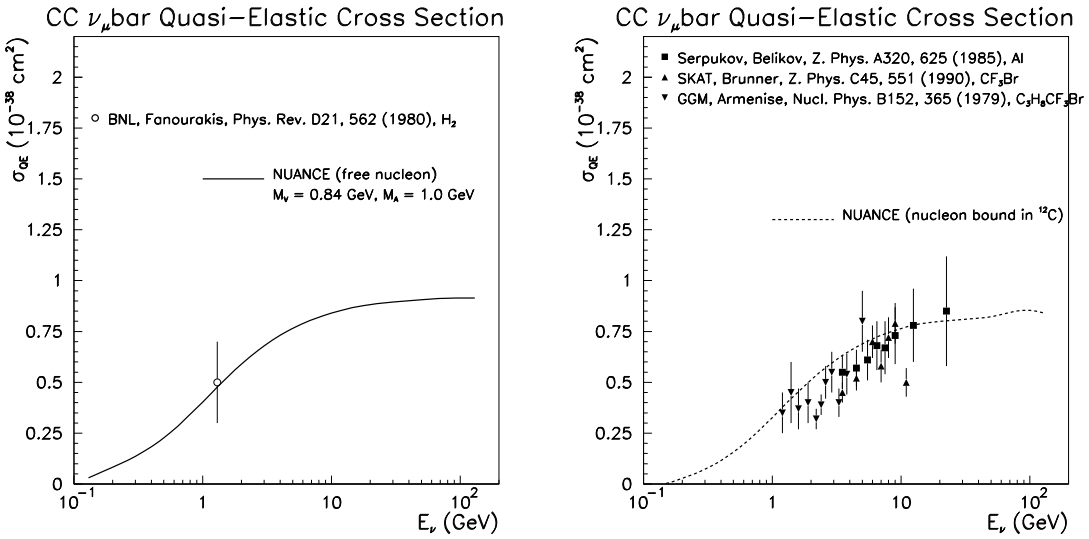

Figure 3.4: *Existing experimental measurements of antineutrino QE scattering cross sections ($\bar{\nu}_\mu p \to \mu^+ n$) off light (left) and heavy (right) targets. The curves indicate the predictions from the NUANCE Monte Carlo generator [7].*

$< E_{\bar{\nu}} >$	Experiment	target	date	# $\bar{\nu}_\mu$ QE events
2 GeV	Gargamelle [12]	$C_3H_8CF_3Br$	1979	766
1.3 GeV	BNL [13]	H_2	1980	13
16 GeV	FNAL [14]	NeH_2	1984	405
6-7 GeV	SKAT [15]	CF_3Br	1988	92
9 GeV	SKAT [16]	CF_3Br	1990	159
5-7 GeV	SKAT [17]	CF_3Br	1992	256

Table 3.4: *Chronological listing of previous $\bar{\nu}_\mu$ QE cross section measurements.*

MiniBooNE expects approximately 40,000 QE interactions in antineutrino mode with 2×10^{20} POT before cuts (to be compared to 766 events from the next most sensitive measurement). Applying the same QE event selection criteria as in our neutrino data [18], yields a sample of $\sim 19,000$ events, 75% of which are pure QE interactions ($\nu_\mu + \bar{\nu}_\mu$ QE). Roughly 23% of the events are neutrino wrong-sign interactions and $\sim 18\%$ are non-QE $\bar{\nu}_\mu$ background events (Table 3.5).

Assuming the wrong-sign constraint from Section 3.1.2 along with conservative errors on the incoming neutrino flux, the background contributions, and event detection together imply that MiniBooNE can measure the antineutrino QE cross section to better than 20% with 2×10^{20} POT. Hence, even with one year of running, MiniBooNE can obtain an order of magnitude more $\bar{\nu}_\mu$ QE events than previous experiments, and be the first to measure the antineutrino QE cross section in this energy range.

Event type	# events passing CC QE selection
CC QE $\bar{\nu}_\mu$ (RS)	10,893
CC QE ν_μ (WS)	3,332
1π $\bar{\nu}_\mu$ backgrounds	3,341
1π ν_μ backgrounds	1,032
QE $\bar{\nu}_\mu$ hyperon production	329
total	18,927

Table 3.5: *Events passing the CC QE event selection in $\bar{\nu}$ mode with 2×10^{20} POT.*

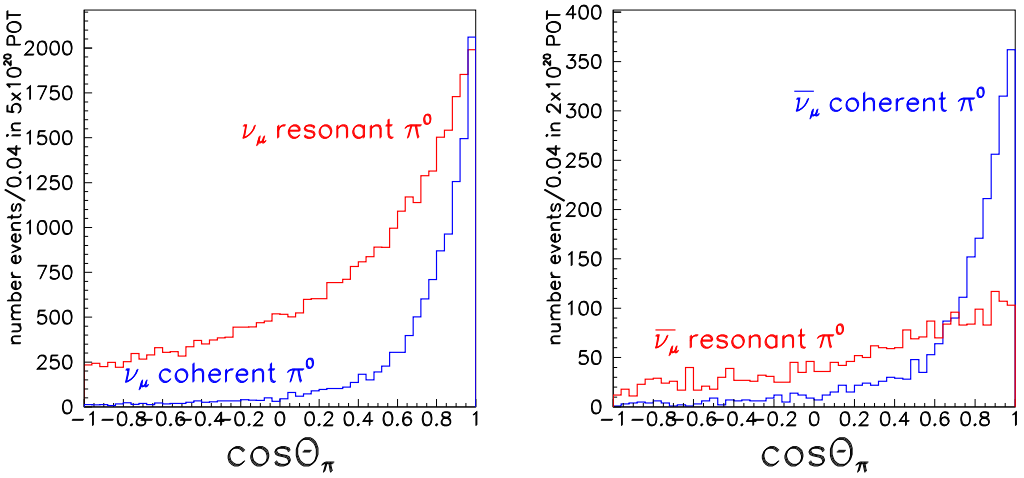

Figure 3.5: *Generated π^0 angular distributions for NC ν (left) and $\bar{\nu}$ (right) scattering [7]. This is the angle of the outgoing π^0 in the lab with respect to the ν direction.*

3.1.4 NC π^0 Production ($\bar{\nu}_\mu N \to \bar{\nu}_\mu N \pi^0$)

To date, there is only one published measurement of the absolute rate of antineutrino NC π^0 production, the single largest background to future $\bar{\nu}_\mu \to \bar{\nu}_e$ oscillation searches; this measurement was reported with 25% uncertainty at 2 GeV [19]. In addition, recent results from MiniBooNE [20] and K2K [21] have renewed interest in the relative rate of coherent versus resonant NC π^0 production. Current theoretical models on coherent π^0 cross sections at low energy can vary by up to an order of magnitude in their predictions [22, 23]. Antineutrino scattering is uniquely suited to improve upon these constraints given that resonant contributions decrease, while coherent production remains the same [22, 23]. This effectively amplifies the coherent contribution. Because coherently produced pions are emitted in the very forward direction, the relative resonant to coherent rate is revealed in the observed pion angular distributions. Figure 3.5 contrasts these distributions for neutrino and antineutrino interactions. In the neutrino case, the fraction of coherent $1\pi^0$ events is half that in antineutrino mode. The coherent contribution is far more dramatic in the antineutrino data, thereby allowing a better measurement of the coherent NC π^0 cross section.

Using the same cuts as in neutrino mode with no further optimization results in

a clean sample of antineutrino NC π^0 events with a similar event purity and efficiency [20]. After this selection, we expect 1,650 $\bar{\nu}_\mu$ resonant NC π^0 events and 1,640 $\bar{\nu}_\mu$ coherent NC π^0 events assuming an exposure of 2×10^{20} POT. Figure 3.6 shows that the amplification of the coherent scattering component clearly persists even after reconstruction and event selection. Also displayed in the figure is the irreducible expected background of roughly 1,000 ν_μ NC π^0 events. Their relative contribution will be well predicted given the constraints on the wrong-sign content in the beam as described in Section 3.1.2 and the measurement of the ν_μ NC π^0 cross section from MiniBooNE neutrino data. Having more (doubling) antineutrino statistics will be important for extracting the antineutrino coherent π^0 measurement, especially given the more complicated template fit in the antineutrino case because of the WS contamination.

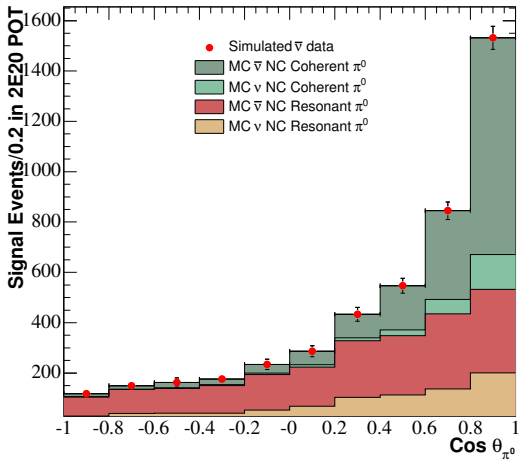

Figure 3.6: *Reconstructed π^0 angular distributions for events passing the NC π^0 event selection in $\bar{\nu}$ mode. Shown are the individual contributions from both $\bar{\nu}_\mu$ and ν_μ resonant and coherent NC $1\pi^0$ production for this mode of running. The errors on the simulated $\bar{\nu}$ data include both statistical and fit uncertainties.*

An accurate determination of the NC π^0 misidentification rate for ν_e and $\bar{\nu}_e$ is required for oscillation searches at the next generation long baseline neutrino experiments. For the MiniBooNE ν_e appearance search we have found that knowledge of the π^0 momentum distribution is crucial and this will continue to be true in future oscillation experiments. The accurate prediction of misidentified π^0's requires that the π^0 momentum distribution be well measured so that the Monte Carlo can be corrected. Figure 3.7 shows an example of the π^0 misidentification rates for the neutrino analysis. Two things are noteworthy. First, the data correction to the Monte Carlo significantly softens the π^0 momentum distribution. Second, the number of misidentified events are enhanced at higher momentum, even though there are disproportionately fewer π^0 events. This is due to the higher Lorentz boost which reduces the momentum of the backwards γ to the point where it cannot be reliable reconstructed. Thus, an accurate determination of the π^0 production rates at low momentum (soft spectrum correction), and higher momentum (increased mis-id rates) is required. Table 3.6 shows the π^0 event rates from the neutrino analysis, and the

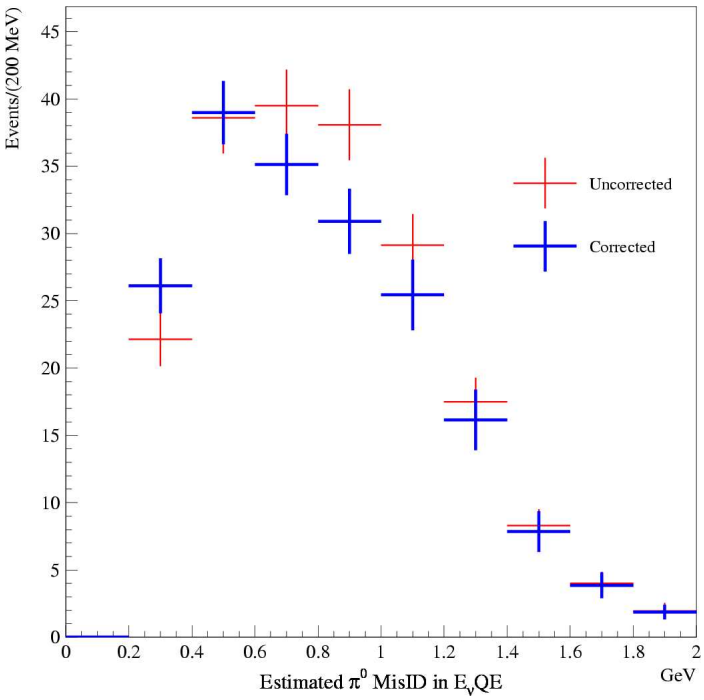

Figure 3.7: *Estimate of the neutrino mis-identification rates from π^0 events in E_ν quasi-elastic energy bins. The red points are the uncorrected Monte Carlo, blue points are after data normalization corrections. Errors include both data statistics and partial systematics, which are almost equal in both cases due to the high π^0 statistics in neutrino mode.*

expected rates for 2×10^{20} and 1×10^{20} POT in antineutrino mode. The biggest concern for the antineutrino analysis is the lack of π^0 events at higher momentum, where the misidentification rate starts to increase. Besides just the raw numbers with statistical errors, a fit to the π^0 mass peak must be done to extract the rates, which are shown for the neutrino case in Table 3.6. Using the significance of the last energy bin in neutrino mode as a benchmark, then with 2×10^{20} POT the analysis would extend to about 0.6 GeV/c in π^0 momentum, while with 1×10^{20} POT it would only extend to 0.5 GeV/c.

3.1.5 CC Resonant Single π^- Production ($\bar{\nu}_\mu N \to \mu^+ N \pi^-$)

In addition to the CC QE and NC $1\pi^0$ cross section measurements that can be made in antineutrino running at MiniBooNE, further exploration of CC resonant pion production rates is equally valuable. Because of the differing isospin content of the final states, the resonances produced in neutrino and antineutrino scattering are distinct (Table 3.7).

Measuring resonant production in antineutrino data allows one to probe the various resonant components. The reaction $\bar{\nu}_\mu p \to \mu^+ p \pi^-$ holds particular interest because it is much more sensitive to the effects of resonances beyond the $\Delta(1232)$, interference between resonances, and non-resonant components. These effects are weakly constrained by limited antineutrino statistics from decades-old bubble chamber experiments (Table 3.8).

π^0 Momentum bin (GeV/c)	Neutrino mode 5.7×10^{20} POT	Antineutrino mode 2.0×10^{20} POT	Antineutrino mode 1.0×10^{20} POT
$0 < p \leq 0.1$	$1525 \pm 150(9.8\%)$	184 ± 14	91 ± 10
$0.1 < p \leq 0.2$	$10380 \pm 197(1.9\%)$	1171 ± 34	586 ± 24
$0.2 < p \leq 0.3$	$9303 \pm 195(2.1\%)$	878 ± 30	439 ± 21
$0.3 < p \leq 0.4$	$5902 \pm 177(3.0\%)$	549 ± 23	275 ± 17
$0.4 < p \leq 0.5$	$2420 \pm 138(5.7\%)$	220 ± 15	110 ± 11
$0.5 < p \leq 0.6$	$1249 \pm 110(8.8\%)$	148 ± 12	74 ± 9
$0.6 < p \leq 0.8$	$913 \pm 90(9.8\%)$	72 ± 9	36 ± 6
$0.8 < p \leq 1.0$	$265 \pm 65(24\%)$	36 ± 6	18 ± 4
$1.0 < p \leq 1.5$	$180 \pm 67(37\%)$	30 ± 6	15 ± 4
Total	$32139 \pm 422(1.3\%)$	3288 ± 57	1644 ± 41

Table 3.6: *Estimated π^0 events in momentum bins for neutrino mode, and two antineutrino cases. The errors for the antineutrino cases are statistical only. The errors on the neutrino mode are statistical and fit errors (brackets are percent errors). The blowing up of errors in high momentum bins will get significantly worse for both antineutrino cases, with an analysis cutoff at 0.6 GeV/c for 2.0×10^{20} POT and 0.5 GeV/c for 1.0×10^{20} POT.*

neutrino type	CC 1π channel	dominant resonance
ν	$\nu_\mu p \to \mu^- p \pi^+$	Δ^{++}
ν	$\nu_\mu n \to \mu^- p \pi^0$	Δ^+
ν	$\nu_\mu n \to \mu^- n \pi^+$	Δ^+
$\bar{\nu}$	$\bar{\nu}_\mu n \to \mu^+ n \pi^-$	Δ^-
$\bar{\nu}$	$\bar{\nu}_\mu p \to \mu^+ n \pi^0$	Δ^0
$\bar{\nu}$	$\bar{\nu}_\mu p \to \mu^+ p \pi^-$	Δ^0

Table 3.7: *CC resonant single pion production modes for neutrino and antineutrino scattering. The dominant contributing baryonic resonance is indicated in each case.*

At MiniBooNE, roughly 7,000 resonant CC $1\pi^-$ events are expected with 2×10^{20} POT before cuts. Although most of the emitted π^-'s will be captured by carbon nuclei, such events still produce a signature: two Čerenkov rings (one each from the μ^+ and π^-) and one Michel electron from the muon decay. While promising, the selection efficiency and purity of such events is unknown at this time. Further investigation is currently underway.

3.2 Oscillation Searches

In addition to cross section advancements that can be made with 2×10^{20} POT of antineutrino running at MiniBooNE, several important oscillation scenarios can also be explored. These include $\bar{\nu}_\mu$ disappearance and $\bar{\nu}_\mu \to \bar{\nu}_e$ appearance searches.

3.2.1 $\bar{\nu}_\mu$ Disappearance

In sterile neutrino oscillation models, the rate of $\overset{(-)}{\nu}_\mu$ disappearance can be significantly larger than $\overset{(-)}{\nu}_\mu \to \overset{(-)}{\nu}_e$ appearance. Therefore, this search has the potential to provide information on additional mixing parameters as well as confirmation of the LSND signal. A disappearance search in antineutrino mode also provides a powerful test of CPT invariance. While CP violation can only be observed in an *appearance* experiment — by observing an asymmetry between the appearance rates in neutrinos and antineutrinos — the appearance mode is unable to distinguish if the asymmetry is the result of CP or CPT violation. As a result, one needs to additionally search for an asymmetry in a *disappearance* experiment. Moreover, the potential for a larger disappearance rate means that a disappearance asymmetry may be observable even if an appearance asymmetry is not.

The MiniBooNE disappearance sensitivity is estimated using the same event selection and systematic errors in neutrino and antineutrino running modes. The event selection results in an 80% pure CC QE sample with 50% efficiency within the fiducial volume [1, 18]. This event selection reflects the current status and will likely improve. The systematic errors in the oscillation fit are dominated by uncertainties on the shape of the neutrino energy distribution, assumed to be 5%. These preliminary systematic errors represent the eventual goals of the ν_μ disappearance analysis.

The resultant MiniBooNE 90% confidence level $\bar{\nu}_\mu \to \bar{\nu}_x$ sensitivity, for 2×10^{20} POT, is shown shown in Figure 3.8 under both CPT conserving (Figure 3.8a) and CPT violating (Figure 3.8b) assumptions. In the CPT conserving case, both ν_μ's and $\bar{\nu}_\mu$'s in the antineutrino data are assumed to oscillate, whereas in the CPT violating case, only $\bar{\nu}_\mu$'s are assumed to oscillate. For comparison, the ν_μ disappearance sensitivity, expected by the end of FY2005, is shown in Figure 3.8a. Only a modest improvement in sensitivity is expected with increased statistics because both the ν_μ and $\bar{\nu}_\mu$ disappearance analyses are systematics limited.

The strongest existing limit on ν_μ disappearance comes from CDHS [30], as shown in Figure 3.8a. However, in the context of CPT violation, this limit does not apply to the $\bar{\nu}_\mu$ disappearance search. In this case, the best $\bar{\nu}_\mu$ disappearance limit comes from CCFR [31], which is much less restrictive and off the scale of Figure 3.8b. As shown, the MiniBooNE $\bar{\nu}_\mu$ disappearance sensitivity in this case extends an order of magnitude lower than the current bounds of $\Delta m^2 \sim 10$ eV^2. In this way, by observing a different rate of ν_μ versus $\bar{\nu}_\mu$ disappearance, MiniBooNE can be directly sensitive to CPT violation in the neutrino sector.

$< E_{\bar{\nu}} >$	Experiment	target	date	# $\bar{\nu}_\mu p \to \mu^+ p \pi^-$ events
1.5 GeV	Gargamelle [25]	$C_3H_8CF_3Br$	1979	282
5-70 GeV	FNAL [26]	H_2	1980	247
5-200 GeV	BEBC [27]	D_2	1983	300
25 GeV	BEBC [28]	H_2	1986	375
7 GeV	SKAT [29]	CF_3Br	1989	120

Table 3.8: *Listing of previous measurements of CC resonant* $\bar{\nu}_\mu p \to \mu^+ p \pi^-$ *events.*

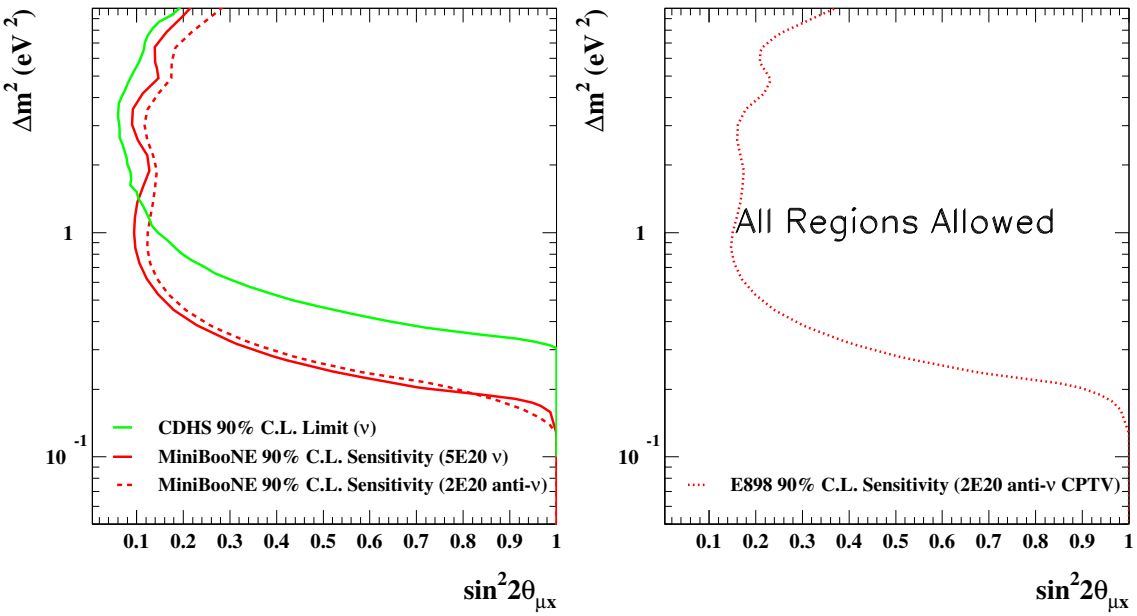

Figure 3.8: *The MiniBooNE 90% confidence level sensitivity under a) CPT conserving and b) CPT violating assumptions. In the CPT conserving case (left), the projected MiniBooNE sensitivity is shown for both $\nu_\mu \to \nu_x$ (with $5{\times}10^{20}$ POT) and $\bar{\nu}_\mu \to \overline{\nu}_x$ (with $2{\times}10^{20}$ POT) oscillations along with the 90% confidence level limit from CDHS [30]. In the CPT violating case (right), only the MiniBooNE $\bar{\nu}_\mu \to \overline{\nu}_x$ sensitivity is shown. In this instance, the existing experimental limits [31] are all above 10 eV^2 and hence the entire region shown on the righthand plot is currently allowed.*

3.2.2 $\bar{\nu}_e$ Appearance

With the potential for CP(T)-violation, testing the LSND oscillation hypothesis in the antineutrino mode in which it was originally observed is imperative (see appendix A for details). In order to make a definitive statement concerning LSND, it will therefore be extremely important for MiniBooNE to search for a signal with antineutrinos at a level sufficient to settle the issue. Although this physics requires more than 2×10^{20} POT, we discuss our preliminary expectations for $\bar{\nu}_e$ appearance here in order to put FY2006/07 running into the context of a larger run plan.

Figure 3.9 shows an estimate of the MiniBooNE sensitivity to $\bar{\nu}_\mu \to \bar{\nu}_e$ oscillations in the scenario in which no $\nu_\mu \to \nu_e$ oscillations occur. In this calculation, a procedure similar to that employed in the 2003 Run Plan [1] was followed, with appropriate adaptations for antineutrinos. Most notably, while in antineutrino mode the number of neutrino interactions ($\bar{\nu}_\mu + \nu_\mu$) per POT is about 29% of the number in neutrino running mode, the intrinsic $\nu_e + \bar{\nu}_e$ background is a comparable fraction of the total event rate in both neutrino and antineutrino running. Here, we compare the sensitivity to the joint KARMEN-LSND region ($\bar{\nu}$ only) [6] as opposed to the full LSND allowed region ($\nu + \bar{\nu}$). This smaller region provides the correct comparison given the difference in neutrino and antineutrino rates possible through CP violation.

Figure 3.9 shows two stops along the path toward decisive resolution of the LSND

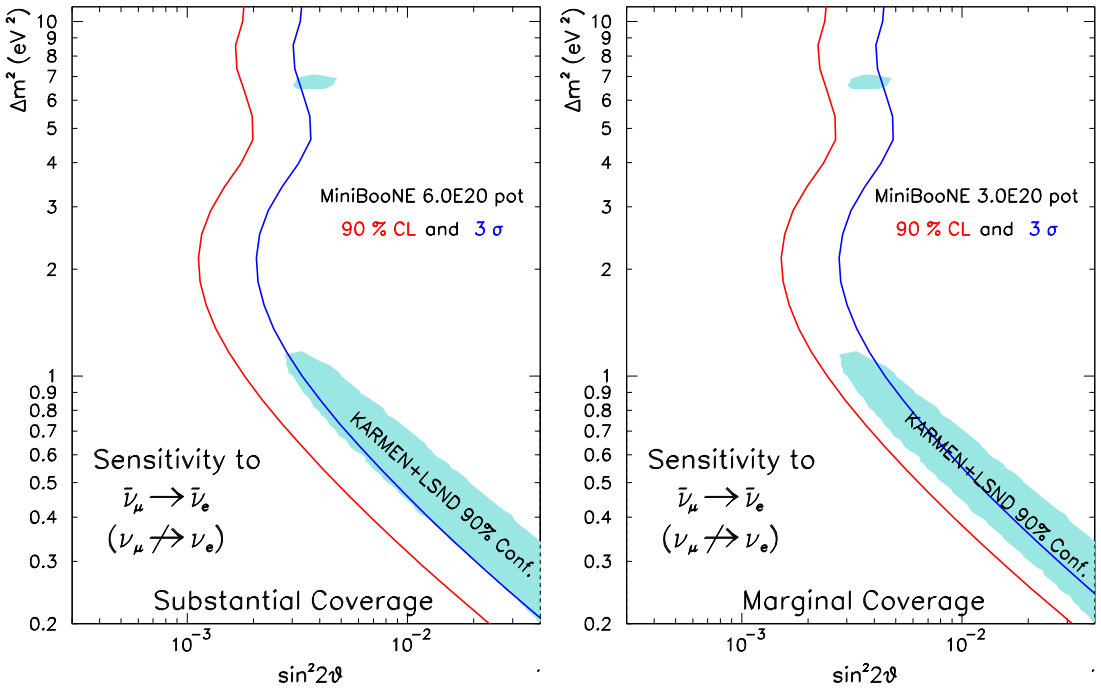

Figure 3.9: *Sensitivity to $\bar{\nu}_\mu \rightarrow \bar{\nu}_e$ oscillations assuming no $\nu_\mu \rightarrow \nu_e$ oscillations using an energy spectrum fit. Shown in blue is the allowed 90% CL region from a joint analysis of the KARMEN and LSND $\bar{\nu}_\mu \rightarrow \bar{\nu}_e$ oscillations results [6]. Left (right) panel shows the result for 6×10^{20} (3×10^{20}) POT.*

question in antineutrino mode. Delivery of 3×10^{20} POT yields marginal (90% CL) coverage of the KARMEN-LSND joint allowed region. 6×10^{20} POT results in substantial (3σ) coverage. This is a statistics-limited search, thus further running will yield an even stronger statement.

Chapter 4

Impact of Oscillation Search Results

4.1 Three Possible Scenarios

We anticipate having a ν_e appearance result in the fall of FY2006 With this result, there are three possible outcomes: 1) a strong signal confirming LSND, 2) an inconclusive result, or 3) a definitive rejection of the hypothesis of LSND-like oscillations in neutrinos. While the objectives of an extended run may differ in each case, the potential for significant scientific output will strongly motivate continued running regardless of the ν_e appearance outcome. A careful consideration of these results will be necessary to determine future run plans. We plan to present new run plans to the PAC in the spring of 2007. However, what follows is a brief discussion of possible future run plans and their justification.

For the moment we have explicitly left out a discussion of how SciBooNE fits into our run plans. Running in antineutrinos is our near term goal and hopefully would fit into the SciBooNE schedule naturally. However, after our neutrino oscillation results become clear, we intend to work in consultation with SciBooNE and the planning office in developing new run plans.

4.1.1 Strong Signal

If MiniBooNE sees a signal, it will be an indication that something interesting and unexpected is occurring in the neutrino sector. It will firmly establish that neutrinos oscillate at three distinct Δm^2 scales. This can only result from new physics such as the addition of one or more sterile neutrinos.

Having established the oscillation with a beam composed primarily of muon neutrinos, the collaboration will work to push this line of research forward on at least two fronts. First, we will begin planning for the construction of additional detectors at different baselines. The number of additional detectors and their baselines will be contingent on the precision and value of our mixing parameter measurements. Second, we will continue running with the existing MiniBooNE detector. Further neutrino running may be needed to better determine the value of the mixing parameters. Alternatively, if we have exhausted the potential of our neutrino data, we will

continue running in antineutrino mode, the objectives of which are outlined in the last chapter, with emphases on oscillation searches.

4.1.2 Inconclusive Result

As discussed in detail in the MiniBooNE Run Plan [1], with less than 1×10^{21} POT, an unfavorable statistical fluctuation in the rates of either signal or background events could shift what would otherwise be a definitive signal (or limit) into an inconclusive result. In this case, the obvious prescription will be to continue accumulating statistics in neutrino mode.

Under certain circumstances, it may be beneficial to reduce the beam decay length by inserting the 25 meter absorber. This configuration change may help address systematic uncertainties due to intrinsic ν_e contamination in the beam.

4.1.3 LSND Excluded in Neutrino Mode

In the case of a definitive exclusion of an LSND-like oscillation in neutrinos, it is essential to search for oscillations in antineutrinos, because, as shown in Section A.1.1, a small (even unmeasurable) oscillation rate in neutrinos does not preclude a sizable rate in antineutrinos. This program has been recognized by the recent APS Interdivisional Neutrino Study [3] as essential to resolving the question of LSND oscillations.

Our intention in this scenario is antineutrino running in FY2006/07 to be the first year in a multi-year $\bar{\nu}_\mu \to \bar{\nu}_e$ oscillation search. In addition to a $\bar{\nu}_e$ appearance search, there exists strong motivation for exploring $\bar{\nu}_\mu$ disappearance as well as an important program of antineutrino cross section measurements. The current knowledge of antineutrino cross sections in the range of 500 MeV to 1.5 GeV is poor, and even a single year of MiniBooNE data at 2×10^{20} POT could yield significant advancement. The physics potential of $\bar{\nu}_\mu$ cross sections measurements, $\bar{\nu}_\mu$ disappearance, and $\bar{\nu}_e$ appearance have been discussed in detail in the previous chapter.

Chapter 5

Conclusions

The LSND evidence for $\bar{\nu}_\mu \to \bar{\nu}_e$ neutrino oscillations is one of the most intriguing issues in particle physics today. If confirmed, the landscape of neutrino physics would be drastically altered, possibly by the addition of a new class of particles in the form of sterile neutrinos or new manifestations of CP violation. MiniBooNE is uniquely positioned to address the LSND result with data successfully taken through January 2006 in neutrino mode. Analysis of the data is in progress, with the goal of producing a first result on $\nu_\mu \to \nu_e$ oscillations in the autumn of 2006.

In this document, we have outlined an important program of antineutrino physics that could be performed with the 2×10^{20} POT expected to be collected. This includes dramatic improvements in our knowledge of $\bar{\nu}_\mu$ cross sections for charged current quasi-elastic scattering and single pion production, and a search for $\bar{\nu}_\mu$ disappearance that would probe significantly further in oscillation parameter space than current limits. The cross section measurements are a necessary prelude to searches for CP violation in neutrino oscillations, including a $\bar{\nu}_\mu \to \bar{\nu}_e$ search at MiniBooNE that could be performed in a longer antineutrino run.

We have currently collected 1×10^{20} POT and request a further 1×10^{20} POT, doubling the statistics, which would improve the measurement of all inclusive modes, but specifically the statistically limited NC π^0 mode. This mode is crucial; an improved production rate measurement as a function of energy will allow a better determination of the electron misidentification background rates, which is of keen interest to future long baseline experiments such as T2K and NOνA.

We ask the PAC to endorse this strong physics program for FY2007 and recommend an extra 1×10^{20} POT in antineutrino mode be delivered to the MiniBooNE beam line. Furthermore, we ask the PAC to recommend that the laboratory continue to pursue a vigorous program to increase proton delivery.

Finally, we would like the opportunity to present a new run plan at the time of the spring 2007 PAC meeting, which will be based on considerations of the neutrino oscillation results.

Appendix A

$\nu_\mu \to \nu_e$ Oscillation Search

A.1 The Physics of LSND Oscillations

The physics motivation for MiniBooNE and a discussion of the theoretical ramifications of LSND oscillations are given in the MiniBooNE Run Plan [1]. One major theoretical insight that has come to light since the Run Plan is the role of CP violation in sterile neutrino models with two or more additional neutrinos [32].

A.1.1 Physics of CP Violating Models

If the LSND signal is due to oscillations, among the best models to explain all data are those which incorporate sterile neutrinos. Models with two or more additional sterile neutrinos (so-called 3+n models) provide a good fit to the data [4] without necessarily violating cosmological bounds.

If more than one Δm^2 contributes to the oscillations, MiniBooNE can be sensitive to a CP violating (CPV) phase in the mixing matrix. Only appearance measurements are sensitive to CPV. This is the motivation for CPV searches at NOνA and T2K, where only the three active neutrinos are generally assumed. In the case of LSND-like oscillations, additional CPV phases may affect the CPV searches both at long and short neutrino oscillation baselines. For example, in 3+2 models [5][32], CPV phases can affect neutrino oscillations in short-baseline experiments, where the oscillation probability is given by:

$$\begin{aligned} P(\overset{(-)}{\nu}_\mu \to \overset{(-)}{\nu}_e) \;=\; & 4|U_{e4}|^2|U_{\mu 4}|^2 \sin^2 x_{41} \;+\; 4|U_{e5}|^2|U_{\mu 5}|^2 \sin^2 x_{51} \;+ \\ & 8|U_{e4}||U_{\mu 4}||U_{e5}||U_{\mu 5}| \sin x_{41} \sin x_{51} \cos(x_{54} \mp \phi_{54}) \end{aligned} \tag{A.1}$$

where

$$x_{ji} \equiv 1.27 \Delta m^2_{ji} L/E \quad \text{and} \quad \phi_{54} \equiv arg(U^*_{e4} U_{\mu 4} U_{e5} U^*_{\mu 5}). \tag{A.2}$$

CPV affects the oscillation probability through the interference term appearing in the second line of this equation.

As a consequence of this model, expectations for MiniBooNE neutrino and antineutrino running can be significantly different. Figure A.1 illustrates this result

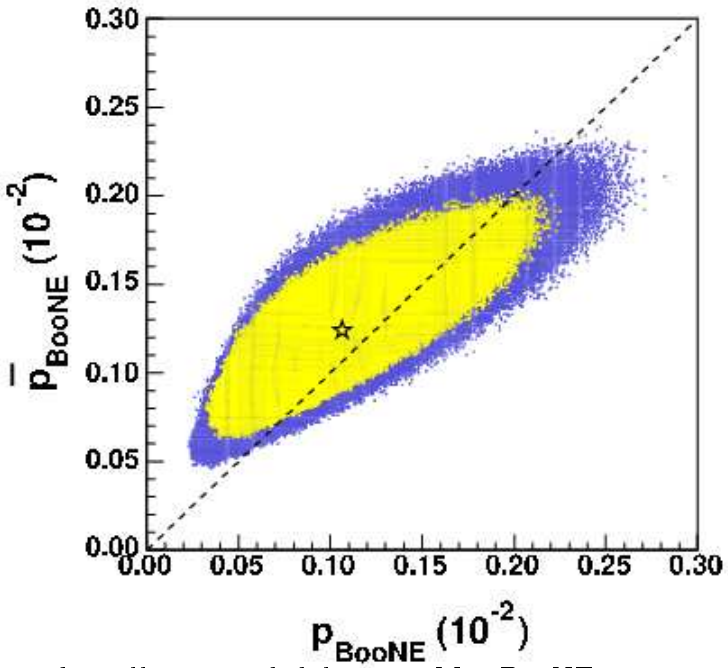

Figure A.1: *Expected oscillation probabilities at MiniBooNE in neutrino and antineutrino running modes, for CP-violating (3+2) models [32]. The yellow region corresponds to the 90% CL allowed region; the blue region corresponds to the 99% CL allowed region.*

for a sampling of 3+2 models with CPV. For each point, there exists at least one combination of masses, mixings, and CPV phase which is consistent with the existing oscillation data, including LSND, at the indicated confidence level. The calculation uses the MiniBooNE neutrino and antineutrino mode fluxes (including ν_e and $\bar{\nu}_e$ backgrounds), thereby taking the energy dependence and wrong-sign neutrino contamination into account. The abscissa is the MiniBooNE oscillation probability in neutrino mode and the ordinate is the oscillation probability in antineutrino mode. One can see that CP violation may enhance or decrease the oscillation probability in antineutrino mode with respect to neutrino mode, depending on the mixing parameters. For small values of oscillation probability in neutrino mode, CPV generally causes an enhancement (of up to a factor two) in antineutrino mode.

Bibliography

[1] A. A. Aguilar-Arevalo *et al.*, "The MiniBooNE Run Plan" (2003).

[2] A. A. Aguilar-Arevalo *et al.*, "Addendum to the MiniBooNE Run Plan: MiniBooNE Physics in 2006" (2006).

[3] "Joint Study on the Future of Neutrino Physics", http://www.aps.org/neutrino (2004).

[4] M. Sorel, J M. Conrad, and M. Shaevitz, Phys. Rev. **D70**, 073004 (2004), *hep-ph/0305255*.

[5] V. Barger, M. Sorel, and K. Whisnant, in preparation.

[6] E. D. Church *et al.*, Phys. Rev. **D66**, 013001 (2002), *hep-ex/0203023*.

[7] D. Casper, Nucl. Phys. Proc. Suppl. **112**, 161 (2002), *hep-ph/0208030*.

[8] G. P. Zeller, proceedings of the 2nd Int'l Workshop on Neutrino-Nucleus Interactions, to be published in Nucl. Proc. Suppl., *hep-ex/0312061*.

[9] T. Suzuki *et al.*, Phys. Rev. **C35**, 2122 (1987).

[10] S. Eidelman *et al.*, Phys. Lett. **B592**, 33 (2004).

[11] M. O. Wascko, proceedings of the 2004 Meeting of the Division of Particles and Fields, to be published in Int. J. Mod. Phys. **A**.

[12] B. Armenise *et al.*, Nucl. Phys. **B152**, 365 (1979).

[13] G. Fanourakis *et al.*, Phys. Rev. **D21**, 562 (1980).

[14] A. E. Asratyan *et al.*, Sov. J. Nucl. Phys. **39**, 392 (1984).

[15] H. J. Grabosch *et al.*, Sov. J. Nucl. Phys. **47**, 1032 (1988).

[16] J. Brunner *et al.*, Z. Phys. **C45**, 551 (1990).

[17] V. V. Ammosov *et al.*, Sov. J. Nucl. Phys. **23**, 283 (1992).

[18] J. Monroe, proceedings of the 39th Recontres du Moriond on Electroweak Interactions and Unified Theories, *hep-ex/0406048*.

[19] see footnote on page 235 in H. Faissner *et al.*, Phys. Lett. **125B**, 230 (1983).

[20] J. L. Raaf, proceedings of the 3rd Int'l Workshop on Neutrino-Nucleus Interactions, to be published in Nucl. Proc. Suppl., *hep-ex/0408015*.

[21] S. Nakayama *et al.*, submitted to Phys. Lett. B, *hep-ex/0408134*.

[22] D. Rein and L. M. Sehgal, Nucl. Phys. **B223**, 29 (1983).

[23] N. G. Kelkar *et al.*, Phys. Rev. **C55**, 1964 (1997); J. Marteau *et al.*, *hep-ph/9906449*; E.A. Paschos and A. V. Kartavtsev, *hep-ph/0309148*; B. Z. Kopeliovich, *hep-ph/0409079*.

[24] S. Adler, Phys. Rev. **135**, B963 (1964).

[25] T. Bolognese *et al.*, Phys. Lett. **81B**, 393 (1979).

[26] S. J. Barish *et al.*, Phys. Lett. **91B**, 161 (1980).

[27] D. Allasia *et al.*, Z. Phys. **C20**, 95 (1983).

[28] P. Allen *et al.*, Nucl. Phys. **B264**, 221 (1986).

[29] H. J. Grabosch *et al.*, Z. Phys. **C41**, 527 (1989).

[30] F. Dydak *et al.*, Phys. Lett. **B134**, 281 (1984).

[31] I. E. Stockdale, C. Haber *et al.*, Zeit. Phys. **C27**, 53 (1985); I. E. Stockdale, C. Haber *et al.*, Phys. Rev. Lett. **52**, 1384 (1984).

[32] G. Karagiorgi *et al.*, arXiv:hep-ph/0609177.